Nuclear Electric Propulsion for Uranus Missions Parametric Assessment

Adam Boylston[1], Sean Greenhalge[2], and Matthew Duchek[3]
Analytical Mechanics Associates, Inc., Denver, CO, 80021, U.S.A.

Nuclear Electric Propulsion (NEP) is an exciting technology that has potential to enable low-thrust missions to Uranus that are otherwise impossible using traditional chemical propulsion. NEP provides enhanced mission flexibility by opening launch windows for such missions and can improve the mass available for payload or propellant at destination while providing power for use in propulsion and communications. This paper investigates the mission trade space, illustrates the tradeoff between time of flight and the usable mass at destination, and considers the effect of different NEP system mass per power on mission performance and optimal propulsion power. The lower-performing NEP systems deliver a comparable mass to Uranus as Uranus Orbiter Probe study from NASA's Decadal Survey, around 250 kg. The higher-performing NEP systems enable payloads up to 1,250 kg which is sufficient for extensive maneuvering in the Uranus system but could also be used for scientific instruments.

I. Introduction

Nuclear Electric Propulsion (NEP) provides a constant source of electric power independent of the sun and at higher power levels than practical for a radioisotope thermoelectric generator (RTG). This capability can enable novel missions to the outer solar system. NEP has a low technology readiness level, with subsystems at various levels of technology completion. NASA's fission surface power (FSP) project is advancing much of the technology, including the reactor and power conversion system, needed to make a 10's of kW-class NEP system. The NEP system in this paper leverages FSP investment, assuming the same high-assay, low enriched Uranium (HALEU) reactor type as the FSP project [1] and considers some improvement in system mass realized through continued technology development by NASA's Space Nuclear Propulsion Program [2], [3]. A range of mass per power values for the NEP vehicle are considered given the uncertainty in the result of future technology development. Similar power levels to the FSP project are used: 10 – 40 kW_e. At this range of power, NEP systems have the potential to reduce transfer times, increase launch window flexibility, and increase payload mass. The increased payload can be used for scientific instruments or propellant, which enables landers, moon tours, and even sample returns. NEP systems will also provide electric power for science upon arrival which presents an exciting opportunity for new science missions to these planets considering that current thermoelectric generators are limited to hundreds of watts.

This paper primarily focuses on the outbound trajectory selection and resulting spacecraft/payload masses of the NEP system. Recent discussions with planetary scientists revealed that, relative to previous missions, increased payload capacity does not expand science objectives without a significant increase to the science budget. Instead, reduced transit times, more flexible launch windows, and maneuverability at the destination planet are key priorities [4]. For this reason, this paper includes transit times faster the 13 years found in the Uranus Orbiter and Probe mission concept study [5]. A Falcon Heavy expendable Launch Vehicle (LV) is assumed for this paper. A variety of NEP system mass assumptions and EP thruster options were also analyzed. Similar analysis has been performed for missions to Neptune using similar methodology by other groups [6]. This paper focuses on Uranus and considers a wider range of possible NEP system mass per power. The results illustrate the optimal power to maximize payload for a given NEP power system mass assumption, vehicle mass model, and launch vehicle selection.

[1] Aerospace Engineer, Advanced Projects.
[2] Mechanical Engineer, Advanced Projects.
[3] Engineering Manager, Advanced Projects.

II. Methodology

The first step in analyzing NEP missions to Uranus was selecting what trajectories were of interest. Because launch flexibility was a priority of this study, trajectories with flybys of other planets were avoided. Though these trajectories may be more optimal than ones investigated, they limit the departure windows to specific opportunities. Instead, this paper focuses on trajectories utilizing only Earth Gravity Assists (EGAs), as they provide an opportunity each year. Several flyby sequences to Uranus using EGAs were considered, as described in Table 1.

Table 1. Destination and trajectories.

Destination	Flyby Sequence	# of Flybys	Strengths	Weaknesses
Uranus	Direct	0	Enables fastest TOF missions	Most dependent on LV C_3
	EEU (1-year coast)	1		
	EEU (2-year coast)	1		
	EEEU (1-year, then 2-year coasts before EGA)	2	Least Dependent on LV C_3	3 years of TOF spent near Earth

The direct trajectory does not rely on gravity assists, adding flexibility. Each EGA adds time penalty in exchange for added energy. A direct mission is theoretically the most flexible, if the launch vehicle can provide enough C_3 to put it in a high enough energy Earth orbit at the beginning of the mission. A two-EGA trajectory has the largest time penalty in return for added energy from repeated flybys. The additional C_3 added by the EEEU case did not outweigh the time penalties, but a single EGA did provide benefit.

The combination of NEP and these simplified trajectories can enable extremely flexible missions. However, there are still optimal launch dates to minimize ΔV. Porkchop plots were generated for an Earth – Uranus trajectory to find the approximate dates for an initial guess in a low-thrust trajectory model with realistic C_3 and TOF values. A heavy NEP spacecraft reduces C_3, but EP makes up for the lower C_3 and enables lower $V_{\infty, \text{arrival}}$, leading to a smaller capture burn for Uranus Orbit Insertion (UOI) than a chemical rocket. These launch date guesses were then used to create reference decks for each flyby sequence in Copernicus, a NASA trajectory optimization software [7]. The launch date was left free so that Copernicus could optimize the launch date for a given mission. The optimal launch date for EP will be different than impulsive burns but utilizing the impulsive dates as an initial guess aided in rapid convergence of the model. The reference decks were built to be the starting points for a large, automated sweep over the trade space. Copernicus trajectories were built for every year from 2035 to 2048 and the resulting ΔV was recorded to ensure the selected launch year provided a ΔV representative of missions leaving any time in this window. The differences in ΔV between launch years are shown in Fig. 1 for an EEU trajectory with a two-year coast before the EGA, which will be referred to as the E(2y)EU trajectory. The 2040 launch opportunity of the E(2y)EU trajectory requires about 10.45 km/s of impulsive ΔV. This value is in the middle of the ΔV range above and indicates that 2040 is representative of expected ΔV values for the timeline when NEP vehicles may be ready to launch.

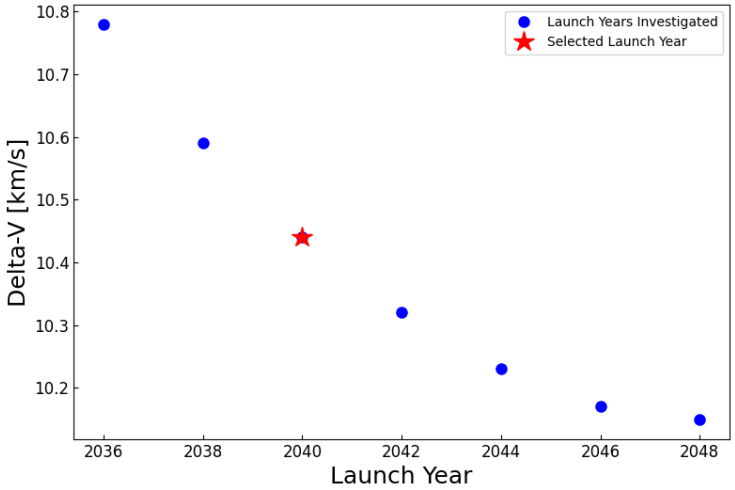

Figure 1. E(2y)EU ΔV vs launch year.

Additionally, a trade study was done to identify the optimal arrival v_∞. This was done by balancing the propellant needed for the chemical UOI burn with the NEP propellant used to slow the spacecraft prior to UOI. A Copernicus deck was created to solve for the needed chemical burn dependent on arrival velocity; a $V_{\infty, \text{arrival}}$ of 2.5 km/s requires a chemical UOI of 210 m/s. For both trajectories the target orbit at Uranus is the same as UOP's arrival orbit: r_a of 5.04E6 km, and r_p of 28,400 km.

The Copernicus deck optimizes the trajectory to minimize power for each launch vehicle C_3, TOF, and I_{sp} of interest. The final mass is fixed at 1000 kg, while the initial mass is left free. This solves for the maximum spacecraft α_{sc}. Here, α_{sc} is defined as the final mass in kilograms per kW jet power. This is not to be confused with α_{ps}, defined above as the mass per power of the NEP power system in kg per kW_e delivered to the thruster PPUs. This approach solves for the maximum delivered mass to Uranus for a given power. However, the maximum delivered mass does not necessarily mean the largest payload. The raw Copernicus data must be post-processed to account for tankage mass of the NEP and chemical propellant and other subsystems that are sized as a function of the spacecraft mass. The lowest power that closes a mission typically will have a higher duty cycle than a mission optimized for a given trajectory to minimize ΔV. The two-year mission above also shows that the spacecraft will have a nearly 100% duty cycle during the EGA, however this drops to about 70% during the interplanetary leg. Figure 2 is a demonstration; for a given TOF, C_3, and I_{sp} the trajectory was solved for a range of possible α_{sc} values, and then post-processed with a given dry mass build up and an assumed α_{ps}.

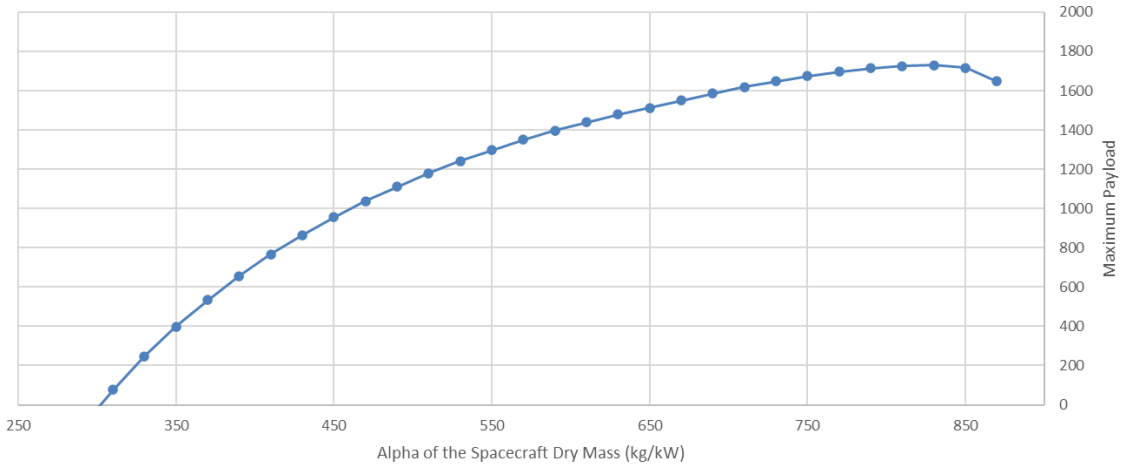

Figure 2. Example maximum payload delivered for an EEU trajectory with an initial C_3 of 21, TOF of 12 years, and I_{sp} of 4000s.

This shows that the minimum power solution – the maximum α_{sc} – is not the highest payload but is close enough to be representative of a possible payload for those parameters, in this case falling within 4%. This shows that the convergence scheme used is valuable in showing trends, as long as it is understood that the payload is representative and not the exact optimal payload. Sweeping for minimum power is much quicker than sweeping across several spacecraft alphas (mass per power) to find the optimum alpha for each mission parameter, while showing overall trends that are accurate.

Initial sweeps in Copernicus were done using an in-house python-based wrapper called CAPYBARA (Copernicus Analysis & Processing for Yielding Batch Astrodynamics Results & Assessments) that iterated each mission's parameters across areas of interest. Initially the range was wide and sparse, but density was added to the trade space parameters as areas of interest were identified. The total range of inputs swept across is shown in the tables below.

Table 2. EU trade space.

	C_3 (km^2/s^2)	TOF (years)	I_{sp} (s)	$V_{\infty, \text{arrival}}$ (km/s)
Minimum Value	20	7	4000	0
Maximum Value	45	17	8000	3

Table 3. E(2y)EU trade space.

	C_3 (km^2/s^2)	TOF (years)	I_{sp} (s)	$V_{\infty, arrival}$ (km/s)
Minimum Value	0	9	4000	0
Maximum Value	30	17	8000	3

The direct trajectory was run to a higher C_3 value and shorter TOF to account for the lack of any EGA. Cases with an EGA require the spacecraft to return to Earth; higher launch C_3's eventually result in diminishing returns as the spacecraft needs to slow for its return. The EEU trade space was narrowed down after some cases were observed to be burning back towards Earth, wasting ΔV in the process. The direct trajectories were also investigated down to 7 years as opposed to 9 years with an EGA due to the EGA adding 2 years to the TOF. Both trajectories were run at 4000 and 8000 s I_{sp} representing the NEXT Ion Thruster [8] and HiPEP Ion Thruster [9], respectively.

The results were post-processed to determine which scenarios were worthwhile for further analysis; the specifics of the post-processing are described later in this section. E(2y)EU – an EGA occurring two years after launch – was selected to run in more detail. The direct EU case, E(1y)EU, and EEEU performed worse than E(2y)EU in the initial results when post-processed using either α_{ps} curve, also shown later in Fig. 5. EU and E(1y)EU did not deliver as large of a payload as E(2y)EU. Shorter TOF was of interest, so the EEEU case spending three years to perform Earth flyby sequences did not allow short times of flight.

With the trajectories narrowed down and a representative launch year chosen, the final versions of the reference decks were created. They are shown below for the EU and E(2y)EU missions.

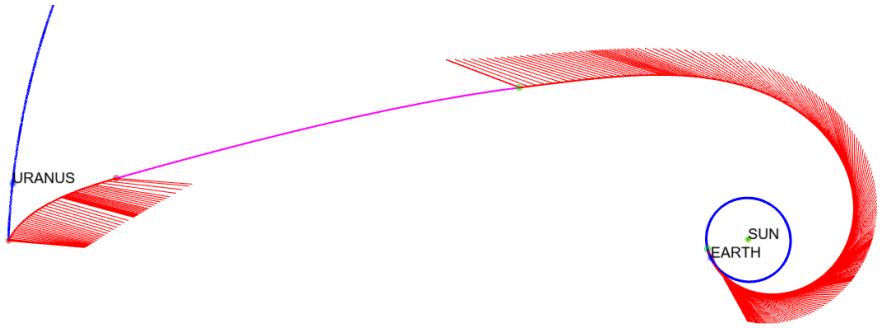

Figure 3. EU example trajectory (C_3 20, TOF 2920 days, I_{sp} 4000s, $V_{\infty, arrival}$ 3 km/s) with thrust direction shown in red.

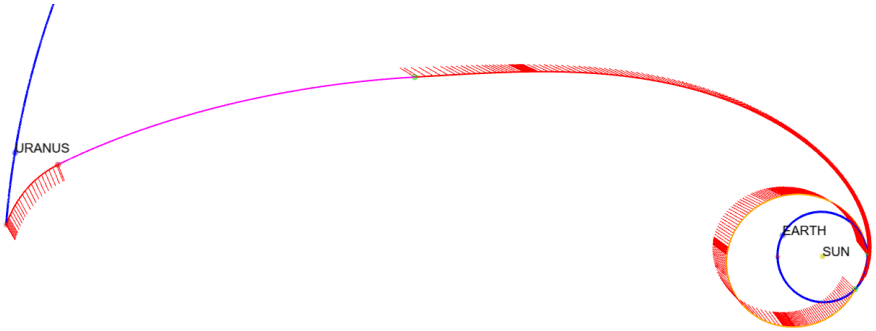

Figure 4. E(2y)EU example trajectory (C_3 20, TOF 4927 days, I_{sp} 4000s, $V_{\infty, arrival}$ 2.5 km/s) with thrust direction shown in red.

The most obvious difference between these two trajectories is the significantly higher thrust required to reach Uranus on the direct trajectory. This is because the direct trajectory is not gaining any additional C_3 from an Earth flyby so it must have a higher thrust level to compensate. The E(2y)EU trajectory gains C_3 from the Earth flyby shown in the picture, however this does limit the range of C3's this mission can be launched with. Above a certain launch energy you burn too far from the Earth to do a two-year EGA and must waste fuel shrinking that orbit.

Once the initial data from the large sweeps is output from CAPYBARA, it is post-processed utilizing an in-house python code OCELOT (Object-oriented CONOPS Evaluation and Logistics Operations Toolkit) designed to scale the

results and estimate the masses of each subsystem. The NEP power system mass is estimated as a function of power using one of the curves in Fig. 5.

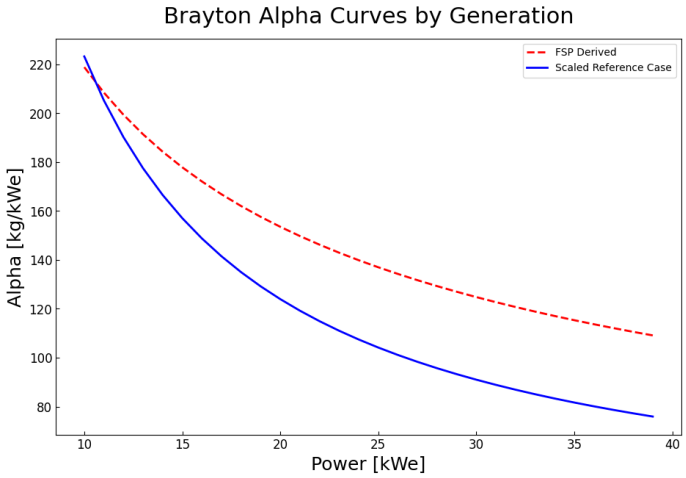

Figure 5. Power system specific mass (α_{ps}) as a function of power. *Two sets of technology choices: 1) derived from FSP reference designs and current investments and 2) scaled around a specific reactor and power conversion point estimate with some improvement from of additional technology investments by NASA SNP.*

Each curve represents the specific mass of NEP power systems with different technology assumptions as a function of electrical power. The 'FSP Derived' curve represents a system directly derived from current technology developments, such as NASA's Fission Surface Power project. The 'Scaled Reference Case' line represents the mass estimate output of a system sizing model of the NEP power system with a specific set of technology assumptions that represent some improvement in performance over the direct FSP-derived system and may result from NASA's ongoing investments by the SNP program. A summary of assumptions used in each NEP generation is shown in the following table.

Table 4. NEP technology choices for parametric specific mass models.

	FSP-derived system	**Additional technology investments by NASA SNP and other programs (Scaled Reference Case** [10]**)**
Reactor	Moderated HALEU	
Reactor Heat Transport Method	Heat pipe/Gas-cooled	Heat pipe
Energy Conversion Cycle	Stirling/Brayton	Re-optimized Brayton for lower sink temp, assumed 2-4% higher-efficiency turbine and compressor
PMAD Voltage	240 V	600 V
PMAD Efficiency	90%	91.2%
Radiator Working Fluid	Water	NaK
Radiator Hot-End Temperature	1100 K	1150 K
Cycle Cold-End Temperature	Optimized to balance mass and radiator area for higher sink temperature	Mass-optimized for deep space sink temperature (colder than FSP Derived)
System Efficiency	~18%	> 20%

The post-processor scales up the initial mass and power until the initial mass matches the launch vehicle capability. This maintains the thrust-to-weight ratio and the validity of the trajectory solution. Subsystem masses are estimated using physics-based sizing for some and component selection for others. Specific hardware was selected for the electric thrusters: NEXT-C Ion thrusters for 4000 s I_{sp} and Hi-PEP Ion thrusters for 8000 s I_{sp}. These are existing thrusters developed by NASA for EP, and the selections represent the most efficient thrusters for their specific impulse. Propellant mass is estimated based on a user-defined ΔV schedule as in Table 5.

Table 5. E(2y)EU ΔV schedule example.

Maneuver	ΔV (m/s)
Earth Departure Burn	3,727
Trans-Uranus Injection Burn	6,094
Uranus Slowdown Burn	3,921
Uranus Orbit Insertion Burn (chemical, impulsive)	210
Moon Tour at Uranus	150
RCS Reserve	75
Total	**14,177**

The power system mass is estimated using the Fig. 5 curves after determining the required electric power by applying thruster efficiency, PPU efficiency, and a performance margin to the scaled jet power. The maximum available payload is determined after a dry mass margin is applied by comparing the calculated mass values to the scaled fixed final mass from Copernicus. The difference between the mass values is interpreted as the available payload. If the available payload is negative (the dry mass exceeds the scaled final mass) then the mission does not close for that launch vehicle at that C_3 for the assumptions made in the spacecraft mass buildup. This means that the assumptions on the NEP system and its mass are key in determining the payload mass that can be delivered.

A sample MEL is shown in Table 6 for a 20 kW_e NEP vehicle using NEXT Ion thrusters launched on a Falcon Heavy Expendable. Mass Growth Allowance (MGA) is applied to the basic mass estimate following the ANSI/AIAA Mass Properties Standard [11]. Additional dry mass margin is kept at the system level, with the total of MGA and margin exceeding 30% of dry mass.

Table 6. Sample MEL, 20 kW_e 4000 s I_{sp} NEP vehicle.

	Basic Mass (kg)	MGA (%)	Predicted Mass (kg)
Power System	2469.3	15	2839.7
Auxiliary Power	234	20	280.8
EP Thrusters and PPU	278.6	10	306.5
EP Tanks and Piping	343.6	20	412.3
RCS Thrusters	5.4	10	5.9
RCS Tanks and Piping	59.7	20	71.6
Structure	650.8	20	780.9
Communications	54	20	64.8
CDH	35	20	42
GNC	97	20	116.4
Thermal	62	20	74.4
Payload	700	0	700
Dry Mass	**4,989.4**	**18**	**5,695.3**
RCS Propellant	651.2	4	677.3
EP Propellant	3,196.7	4	3,324.5
Dry Mass Margin		**18**	**1,025.2**
Wet Mass			**10,722.3**
LV Capability			**10,937.1**
Total Dry Mass Margin	**34.7% (705.9 MGA + 1,025.2 margin)**		

III.Results

Post-processing each combination of NEP system generation and I_{sp} reveals the trajectories that close with a positive payload delivered to Uranus. However, sweeping over three dimensions leads to a difficult to visualize trade space. For simplification only one I_{sp} is plotted at a time. To simplify the data further, a launch vehicle curve can be applied to show only trajectories enabled by a specific launch vehicle. As mentioned previously, a Falcon Heavy Expendable is the focus of this paper due to a combination of high availability and low cost. The maximum payload for each trajectory is found by comparing the wet mass of the spacecraft from the MEL to the available C_3 of the spacecraft. The images below compare the possible payload delivered to Uranus orbit on a direct trajectory for 4000 s NEXT Ion thrusters and 8000 s HiPEP Ion thrusters, both launched on a Falcon Heavy Expendable.

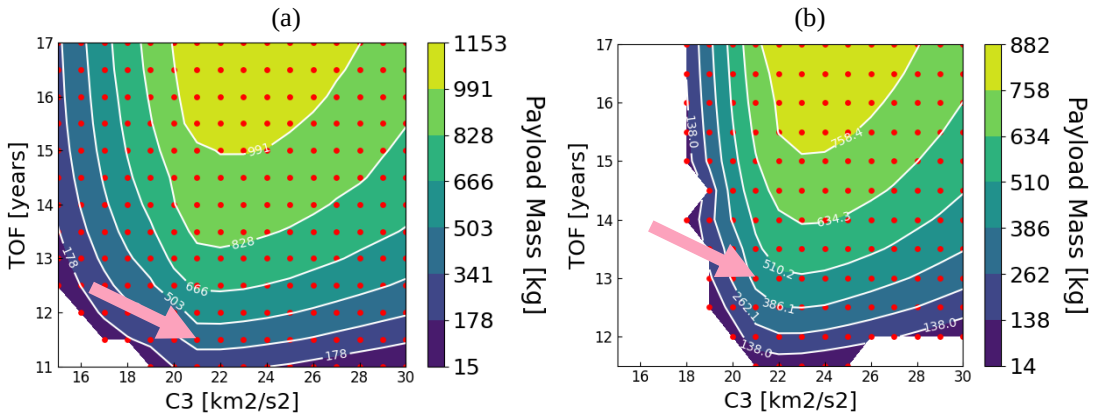

Figure 6. E(2y)EU Maximum Payload with FSP-Derived NEP System at (a) 4000 s and (b) 8000 s I_{sp}.

An FSP derived NEP system using thrusters with an I_{sp} of 4000 s delivers almost 300 kg more than a NEP system that uses 8000 s thrusters for the longest trip times. The launch C_3 at which the maximum payload occurs are roughly the same between the two thrusters, about 24 km^2/s^2. The pink arrows indicate the point in the trade space at which 4000 s thrusters could deliver the same 400 kg payload as 8000 s thrusters 1.5 years faster with the same launch energy.

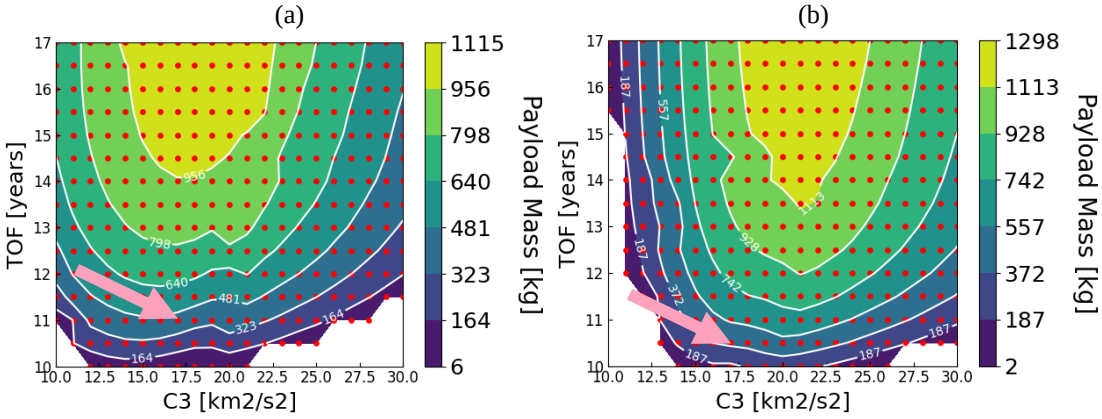

Figure 7. E(2y)EU Maximum Payload with Scaled Reference Case NEP System at (a) 4000 s and (b) 8000 s I_{sp}.

The scaled reference case results are slightly different than the FSP-derived system, with the 8000 s thrusters converging on payloads almost 200 kg higher than 4000 s thrusters for the longest trip times. Despite this, the same trend of 4000 s thrusters enabling lower C_3 trajectories is seen again here due to their higher thrust. In these plots we see the same 400 kg payload pointed out in Fig. 6 is delivered in 11 years with 4000 s thrusters and 10.5 years with 8000 s thrusters. This suggests that the scaled reference case NEP vehicle could reduce transit time by operating at a higher $I_{sp,}$ e.g. by using HiPEP Ion thrusters as opposed to NEXT. The difference between the results using the FSP-derived and 'scaled reference concept' power system specific mass estimates indicates the importance of technology uncertainty to the mission capability result.

The power level of the NEP reactor corresponding to these maximum payloads are shown below, first for FSP-derived NEP at 4000 and 8000 s I_{sp}. Figure 8 shows the minimum power required to deliver the payloads shown in Fig. 6. As C_3 and TOF increase, required power goes down. There is more time for thruster operation, enabling a lower thrust level. The higher I_{sp} 8000 s system requires higher power to optimize the same trajectories due to its lower thrust for a given power level.

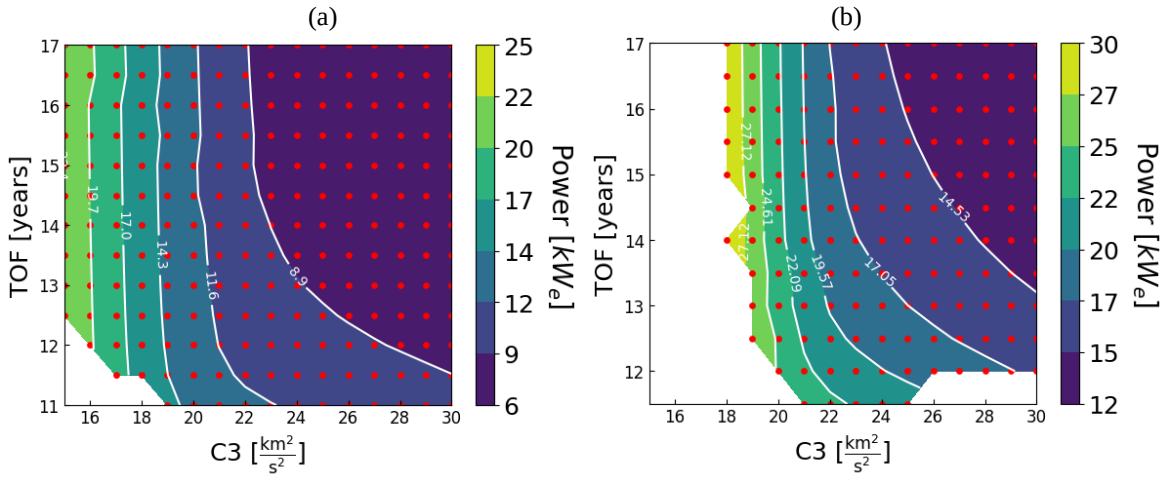

Figure 8. E(2y)EU minimum power of FSP-Derived NEP system at (a) 4000 s and (b) 8000 s I_{sp}.

Figure 9 shows the minimum power required to deliver the payloads shown in Fig. 7. Earlier it was shown that the scaled reference case NEP vehicle operating at 8000 s delivers more payload than at 4000 s. These contours show that it does this with a higher power reactor, taking advantage of the lower α_{ps} compared to the directly FSP-derived system.

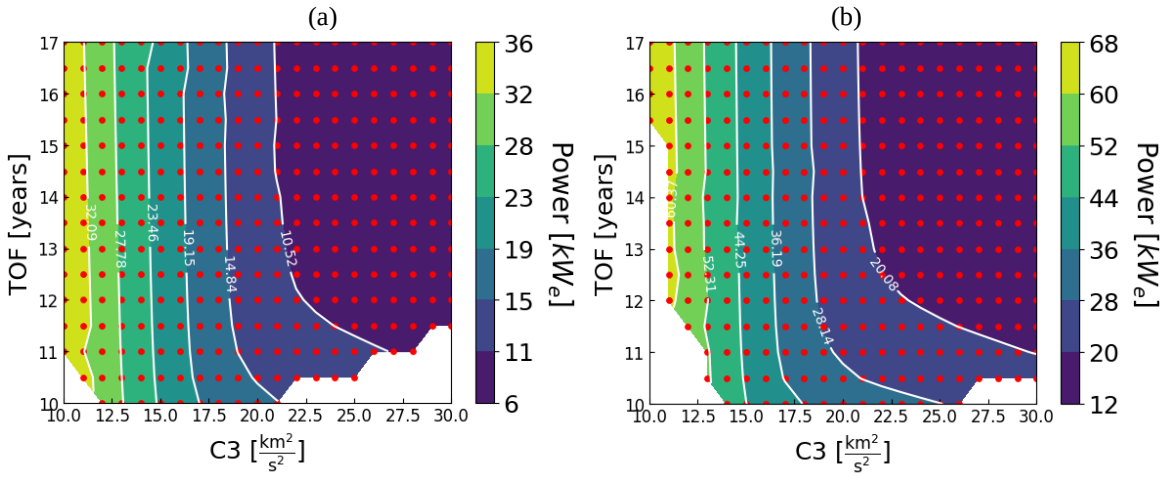

Figure 9. E(2y)EU minimum power of scaled reference design NEP system at (a) 4000 s and (b) 8000 s. I_{sp}

In Fig. 10, the maximum payload is plotted as a function of TOF for each of the two power system specific mass assumptions originally given in Fig. 5. Two design points from the Uranus Orbiter Probe study are included for comparison.

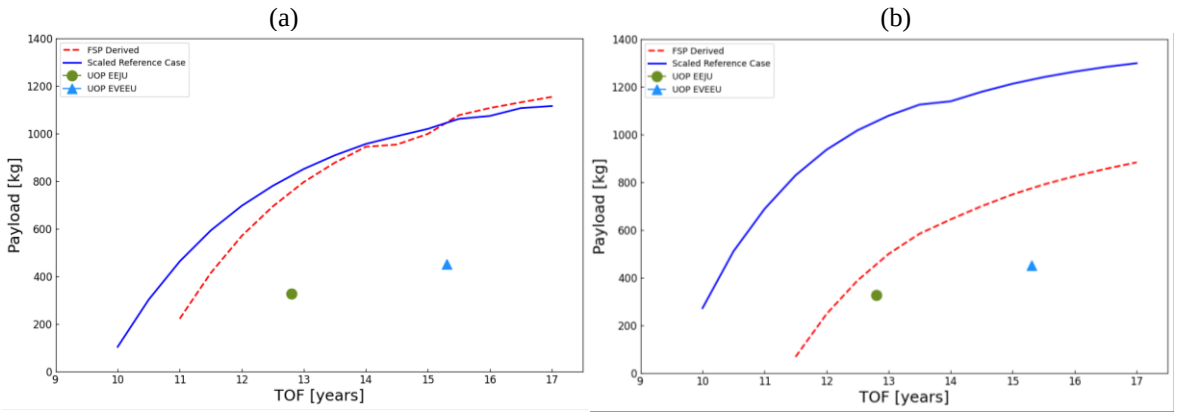

Figure 10. E(2y)EU maximum payload of scaled reference case NEP system at (a) 4000 s and (b) 8000 s I_{sp} with comparison to FSP-Derived system.

The figures above show that regardless of TOF, I_{sp}, and even NEP generation, NEP can deliver more payload than UOP. Even at shorter TOFs than UOP's trajectory NEP could deliver up to 3 times the payload mass. The UOP payload utilizing an EEJU trajectory could be delivered by the scaled reference case NEP system in about 10.5 years at 4000 s I_{sp} and 10 years at 8000 s, compared to 13 and 15 years for the two UOP points. For the scaled reference case system, an I_{sp} of 8000 s delivers more payload than 4000 s at every TOF, however that is associated with higher power levels as discussed previously.

The required ΔV for 4000 s and 8000 s thrusters for both the FSP-Derived and scaled reference design NEP vehicles is plotted in Figs. 11 and 12.

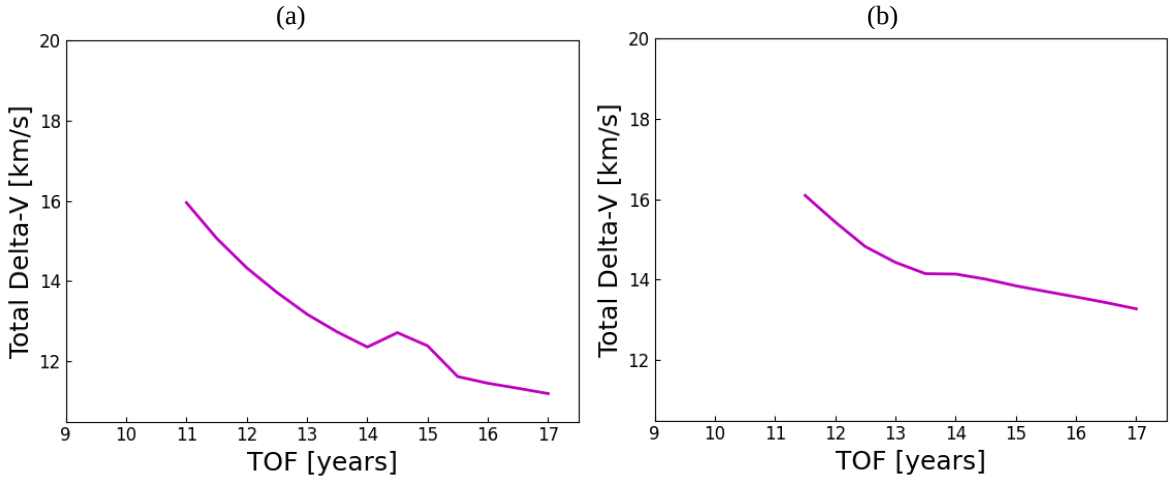

Figure 11. E(2y)EU ΔV for maximum payload of FSP-Derived NEP system at (a) 4000 s and (b) 8000 s I_{sp}.

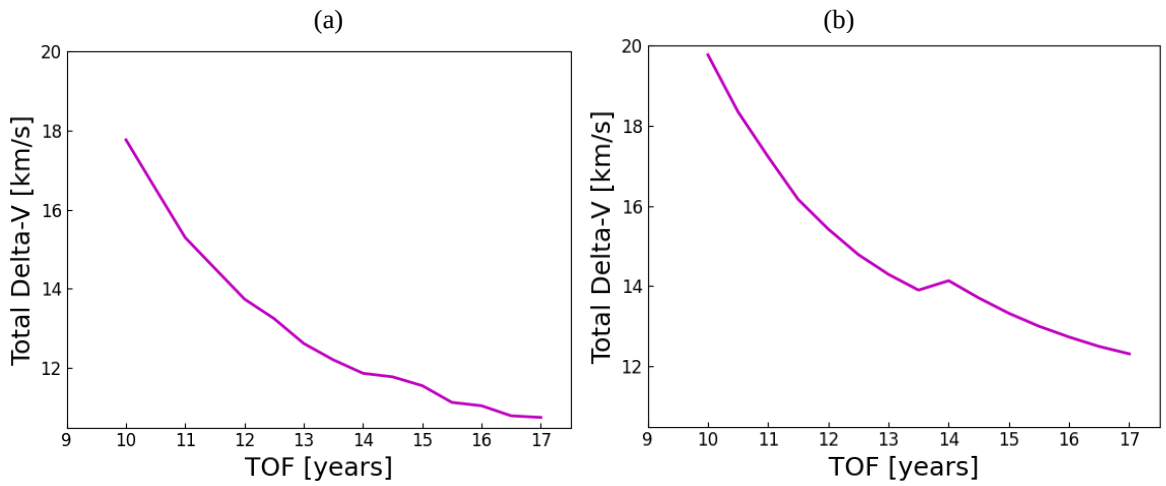

Figure 12. E(2y)EU ΔV for maximum payload of scaled reference case NEP system at (a) 4000 s and (b) 8000 s I_{sp}.

All four plots show the same trend of ΔV decreasing as TOF increases. A shorter TOF allows the trajectory to be more optimal as it becomes closer to a Hohmann transfer versus more of a shortcut trajectory. 8000 s is shown to require more ΔV than 4000 s which tracks with its associated higher power shown before. Moving from an FSP derived system to the scaled reference case NEP system sees roughly a 1 km/s ΔV decrease across all TOFs at 4000 s. At 8000 s the differences are larger at the extremes of TOF, but the ΔV requirements are approximately equal from 12 to 14 years.

IV. Discussion and Conclusion

This paper demonstrates potential missions to Uranus across a range of NEP systems. Due to the uncertain nature of the performance of these systems, a range of power, α_{ps}, and I_{sp} values were investigated. To investigate this the large trade space, a parametric approach to the mission analysis was used to allow determination of delivered usable mass as a function of TOF for a range of chosen power system and spacecraft assumptions.

With the NEP system mass per power estimates considered, a payload and flight time similar to the Uranus Orbiter and Probe decadal survey mission study is possible while also delivering significant propellant for maneuvering in the Uranus system. The NEP system may enable new science by providing kilowatts of power and thus data rate from the Uranus system, as well as additional maneuverability compared to a chemical system. With a NEP system with some performance improvement beyond a direct FSP-derived system (the scaled reference case in Fig. 5), a higher-I_{sp} thruster system provides benefit in terms of additional mass deliverable for a given flight time. This system provides ample delivered mass for payload and propellant to enable maneuvers with significant ΔV requirements, such as plane changes and spiraling in/out of moon orbits. This capability would enable new mission designs as well as high communication data rates for a different instrument suite selection. A 20 kW_e system with modest improvement over an FSP-derived system provides enough delivered mass that a compelling mission may be designed.

For any of the power system performance levels considered, there remain significant challenges to be overcome in the technology development. These include long-life power conversion that must operate for the full 12- to 18-year mission, including operations at Uranus. It is worth noting that a lower-mass power system enables a shorter Earth-Uranus transit time that could relax the life requirement by one to two years compared to the heavier power systems considered. A 12- to 15-year mission may be significantly more attractive than a 14 to 18-year mission.

This analysis should inform NASA's plans for technology development of NEP for science mission applications. A Uranus mission places even more emphasis on low mass and long operational life than do current developments for fission surface power. Additionally, the analysis here illustrates that the optimal power level for an ice giant science mission NEP is likely between seven and 30 kW_e, depending on how the reactor concept scales with thermal power, the achieved efficiency of the power conversion system, and the I_{sp} of the thruster used. Off-optimal higher power levels can close the mission with much less penalty than the difference in power system mass due to the lower ΔV possible with higher thrust-to-weight ratio, but there is still significant penalty going to off-nominal power. Different launch and Earth-departure capabilities do have an impact on the optimal power, with more-powerful launch vehicles

favoring larger, higher-power NEP systems. These considerations may drive additional or different technology choices to meet the more demanding mission requirements and may provide justification for a different-scale power system.

Based on the parametric analysis completed, further study and development of a conceptual point design including selection of a science package that takes advantage of the available power at destination is warranted as follow-on work. This is needed to evaluate the degree to which new science is enabled and to more specifically quantify the amount of propulsion needed at destination and the resulting requirement on power system specific mass.

Acknowledgments

This work was supported by NASA's Space Technology Mission Directorate (STMD) through the Space Nuclear Propulsion (SNP) program. Analytical Mechanics Associates, Inc. was funded for this effort under NASA Contract No. 80LARC23DA003.

V. References

[1] L. Mason, L. Kaldon, S. Corbisiero and D. Rao, "Key Design Trades for a Near-term Lunar Fission Surface Power Study," in *Nuclear and Emerging Technologies for Space*, Atlanta, 2025.

[2] K. A. Polzin, A. K. Martin, F. Curran, R. Myers and M. Rodriguez, "Strategy for Developing Technologies for Megawatt-class Nuclear Eletric Propulsion Systems," in *International Electric Propulsion Conference*, Boston, MA, 2022.

[3] M. E. Duchek, W. Machemer, C. Harnack, M. Clark, A. Pensado, K. Polzin, A. Martin, F. Curran, R. Myers, M. Rodriguez, D. V. Rao, R. Dyson and R. Scheidegger, "Key Performance Parameters for MW-Class," in *AIAA ASCEND*, Las Vegas, NV, 2022.

[4] T. Reuter, R. Myers, P. Christensen, L. Dudzinski and K. Polzin, "Accelerating Space Science with Nuclear Technology: The Tempe Workshop," Institute for Space Science and Development, Hastings-on-Hudson, NY, 2023.

[5] A. Simon, F. Nimmo and R. C. Anderson, "Uranus Orbiter & Probe," National Aeronautics and Space Administration, 2021.

[6] T. Kokan, C. R. Joyner, D. J. H. Levack, B. J. Muzek, R. W. Noble and C. B. Reynolds, "Nuclear Electric Propulsion Outer Planetary Science Mission Concepts," in *AIAA SciTech*, Orlando, FL, 2025.

[7] J. Williams, *Copernicus Version 5.2.0,* NASA Johnson Space Center, 2022.

[8] G. C. Soulas, M. T. Domonkos and M. J. Patterson, "Performance Evaluation of the NEXT Ion Engine," in *39th AIAA/ASME/SAE/ASEE Joint Propulsion Conference and Exhibit*, Huntsville, 2003.

[9] J. E. Foster, T. Haag, M. Patterson, G. J. Williams Jr., J. S. Sovey, C. Carpenter, H. Kamhawi, S. Malone and F. Elliot, "The High Power Electric Propulsion (HiPEP) Ion Thruster," in *40th AIAA/ASME/SAE/ASEE Joint Propulsion Conference and Exhibit*, Fort Lauderdale, 2004.

[10] W. Machemer, M. Duchek, C. Harnack, E. Grella, D. Nikitaeva and C. D. Smith, "Mass Modeling of NEP Power Conversion Concepts for Human Mars Exploration," in *Nuclear and Emerging Technologies Conference (NETS)*, Cleveland, 2022.

[11] AIAA, "Standard: Mass Properties Control for Spacecraft ANSI/AIAA S-120A-2015," American Institute of Aeronautics and Astronautics, Reston, VA, 2015.

[12] M. Duchek, A. Boylston, D. Langford, S. Greenhalge, K. Polzin and R. Myers, "Nuclear Electric Propulsion for Outer Planet Science Missions," in *International Electric Propulsion Conference*, Toulouse, France, 2024.